

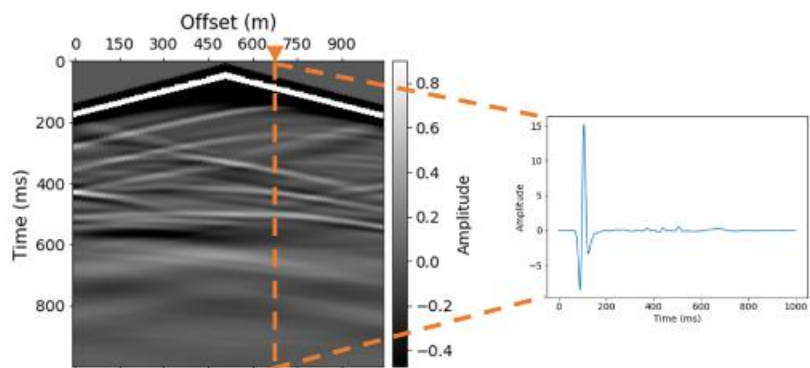


ABA-FWI: Augmented Boundary Attention for Full Waveform Inversion

Qiong Xu^{ID}, Fan Min^{ID}, *Member, IEEE*, Shulin Pan^{ID}, Xing-Yi Zhang^{ID},
Guojie Song^{ID}, Ke Wang^{ID}, and Xindong Wu^{ID}, *Fellow, IEEE*

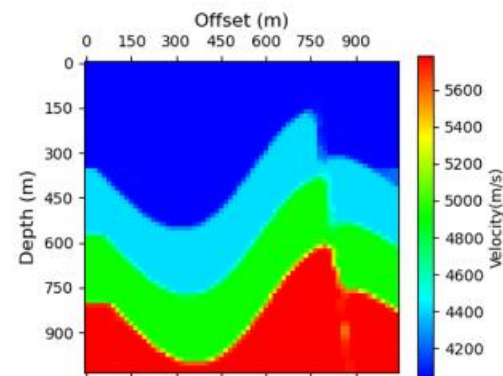
IEEE TRANSACTIONS ON GEOSCIENCE AND REMOTE SENSING 2024

Full Waveform Inversion (FWI)



(b)

Seismic Data p



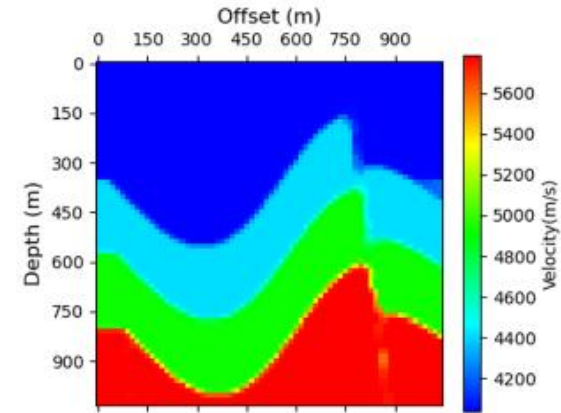
(a)

Velocity Maps c

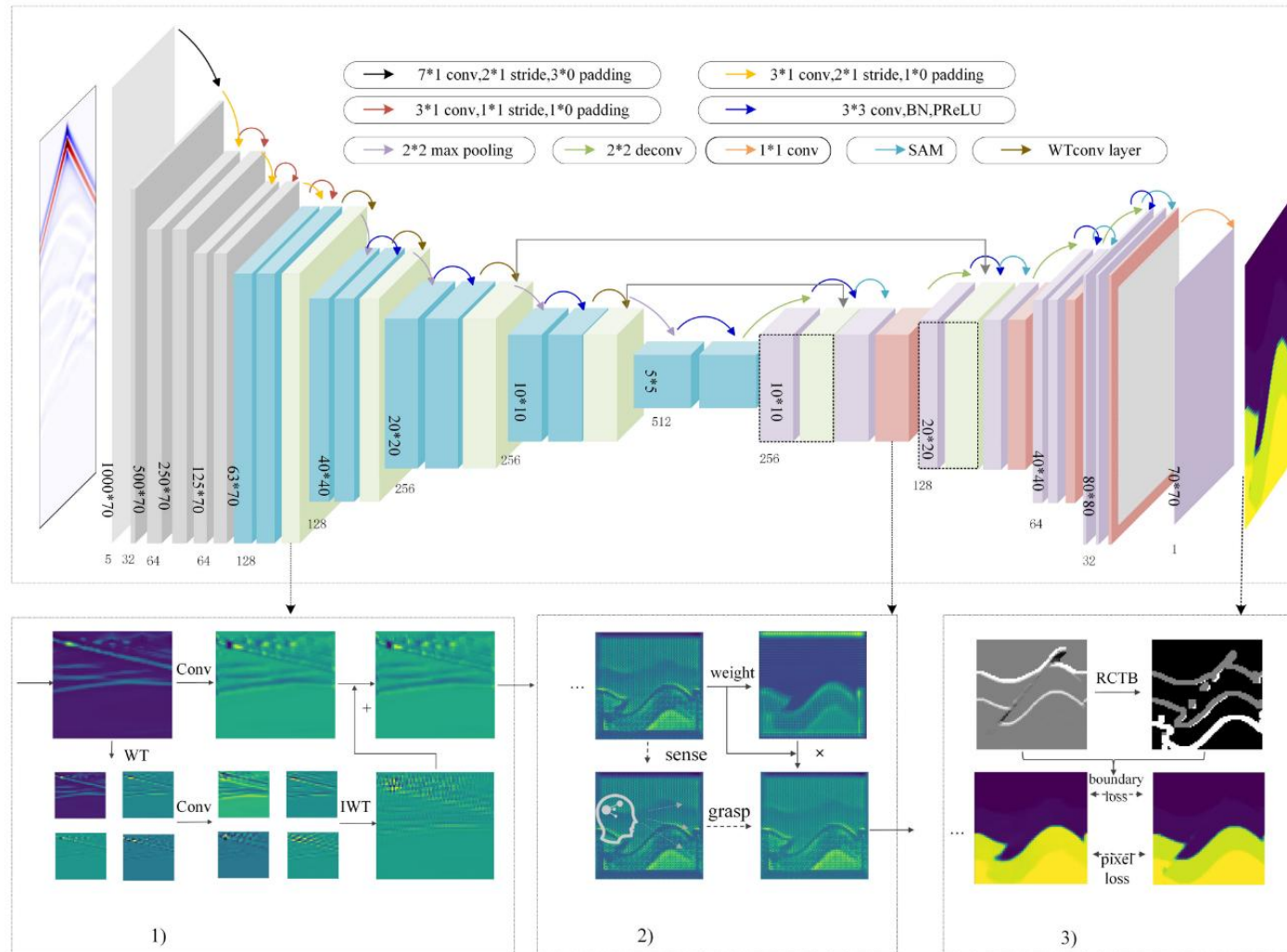
Deep learning full waveform inversion (DL-FWI) is an end-to-end and time-efficient high-resolution imaging technique for subsurface media.

Popular methods are often plagued by location drift and significant velocity misfits at the **stratigraphic boundaries**.

We propose an **augmented boundary attention** algorithm (**ABA-FWI**) to focus on the key boundary information.

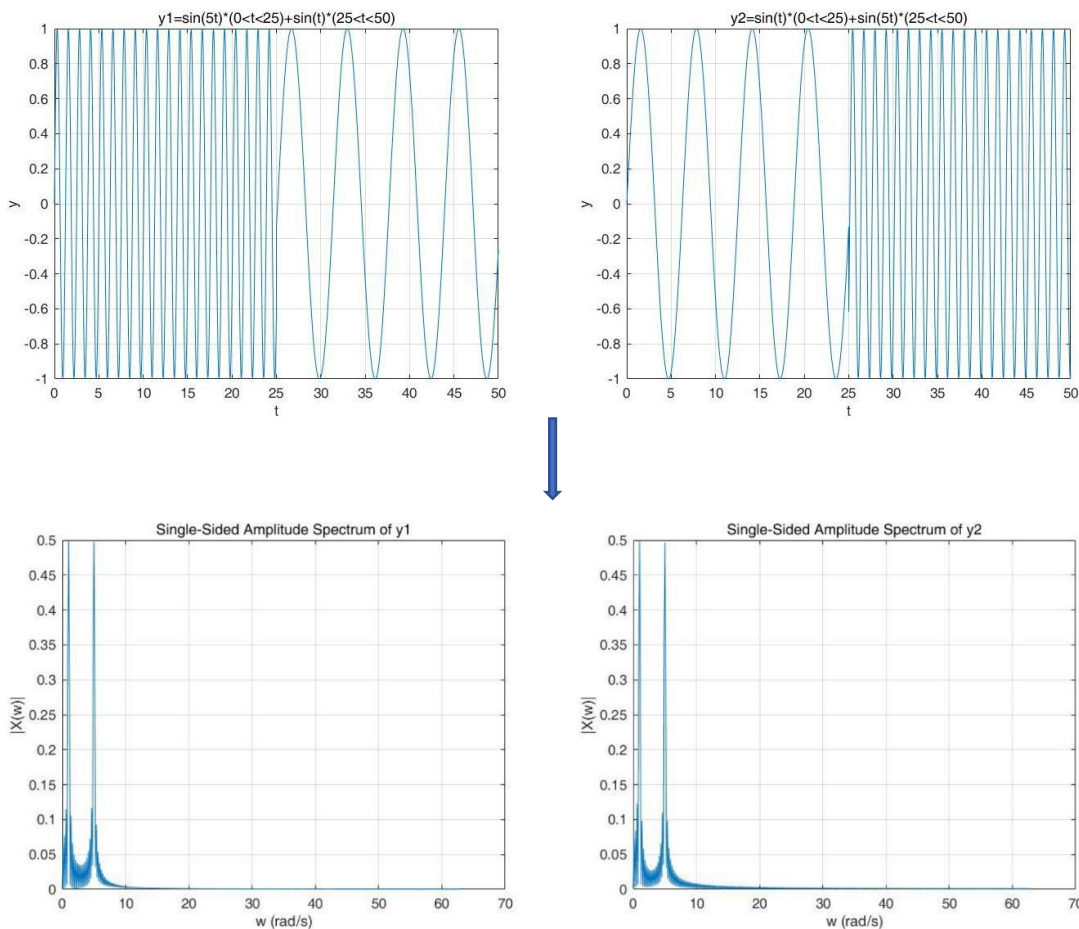


The Architecture of ABA-FWI



Fourier Transformation

非平稳信号：频率内容随时间变化



傅立叶级数：任何周期信号，都可以分解成**离散**频率的正弦和余弦波的叠加

$$f(x) \sim \frac{a_0}{2} + \sum_{n=1}^{\infty} \left[a_n \cos\left(\frac{2\pi n x}{T}\right) + b_n \sin\left(\frac{2\pi n x}{T}\right) \right] = \sum_{n=-\infty}^{\infty} c_n e^{i \frac{2\pi n x}{T}}$$

傅里叶变换的核心思想是信号分解成**连续**频率的正弦和余弦波的叠加，从而将信号从时域（或空间域）转换到频域，不要求周期性。

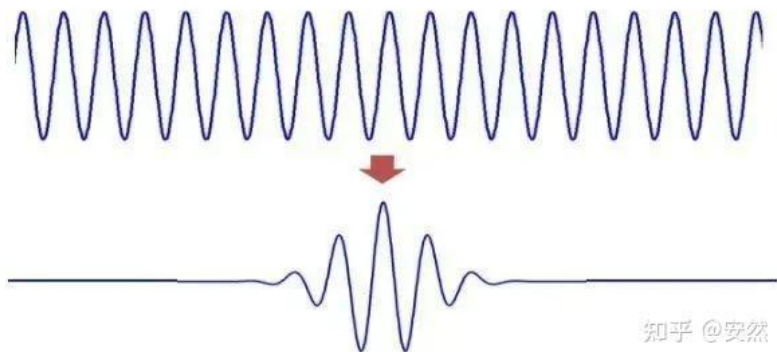
$$F(\omega) = \int_{-\infty}^{\infty} f(t) e^{-i\omega t} dt$$

缺点：实际应用中存在大量的非平稳信号，在将信号从时域变换到频域的时候，丢失了时空信息

Wavelet Transform

小波变换

$$F(\omega) = \int_{-\infty}^{\infty} f(t) * e^{-i\omega t} dt \Rightarrow WT(a, \tau) = \frac{1}{\sqrt{a}} \int_{-\infty}^{\infty} f(t) * \psi\left(\frac{t-\tau}{a}\right) dt$$



小波变换可以理解为用经过缩放和平移的一系列小波函数，代替傅里叶变换的正弦波和余弦波进行傅里叶变换的结果，既包含时域信息又包含频域信息

$$WT(a, \tau) = \frac{1}{\sqrt{a}} \int_{-\infty}^{\infty} f(t) * \psi\left(\frac{t-\tau}{a}\right) dt$$

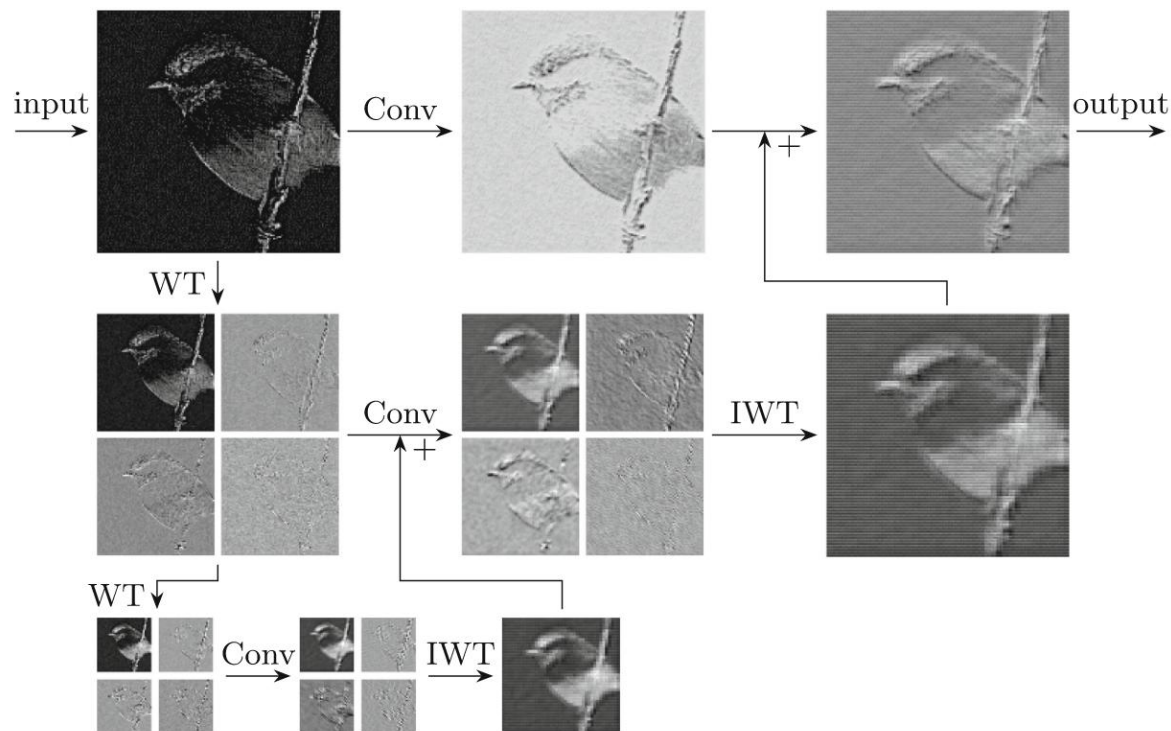
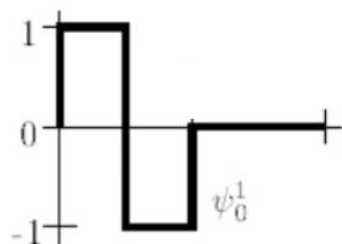
尺度a(scale): 尺度a控制小波函数的伸缩。a就对应于频率（反比）。

平移量τ(translation): 平移量τ控制小波函数的平移，τ就对应于时间。

1. WTconv layer [1]

Haar 小波函数 ψ :

$$\psi(x) = \begin{cases} 1, & \text{for } 0 \leq x < 1/2 \\ -1, & \text{for } 1/2 \leq x < 1 \\ 0, & \text{otherwise} \end{cases}$$

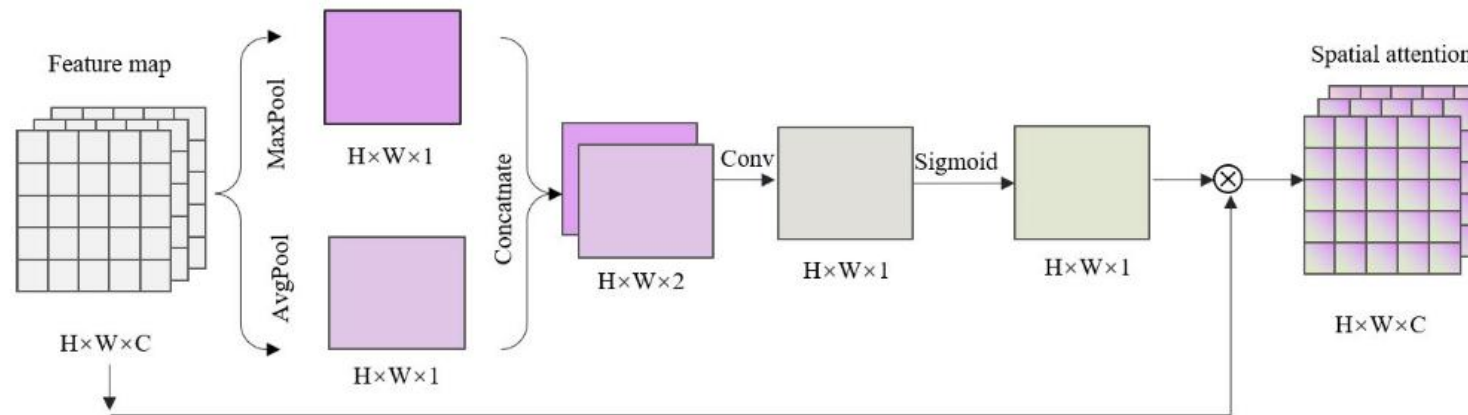


$$f_{LL} = \frac{1}{2} \begin{bmatrix} 1 & 1 \\ 1 & 1 \end{bmatrix}, f_{LH} = \frac{1}{2} \begin{bmatrix} 1 & -1 \\ 1 & -1 \end{bmatrix}, f_{HL} = \frac{1}{2} \begin{bmatrix} 1 & 1 \\ -1 & -1 \end{bmatrix}, f_{HH} = \frac{1}{2} \begin{bmatrix} 1 & -1 \\ -1 & 1 \end{bmatrix}$$

low-frequency

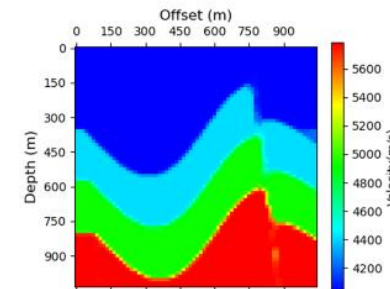
horizontal, vertical, and diagonal high-frequency

2. (spatial attention module) SAM



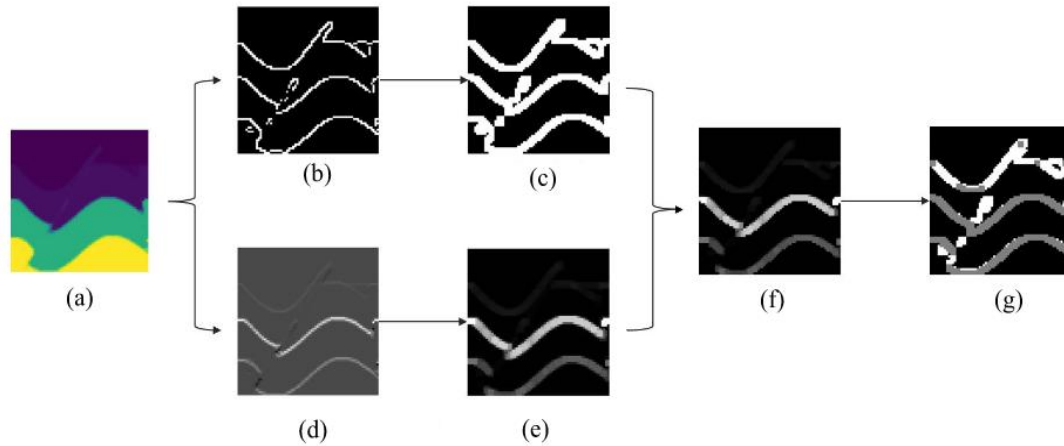
This approach recovers previously neglected spatial information, facilitating precise **boundary localization and clearer delineation** in DL-FWI.

$$\mathcal{L}_{\text{boundary}}(\mathbf{v}, \tilde{\mathbf{v}}) = \frac{1}{nm} \sum_{i=1}^n \sum_{j=1}^m W(\mathbf{v})_{ij} G(\mathbf{v}, \tilde{\mathbf{v}})_{ij}$$



(a)

3. (reflection coefficient tuned boundary) RCTB loss function



$$\text{Canny: } \mathbf{e} = E(\mathbf{v}). \quad (5)$$

$$(\mathbf{e} \oplus \mathbf{k})_{ij} = \max_{(i',j') \in D(\mathbf{k})} \mathbf{e}_{i-i',j-j'} \quad (6)$$

$$R(\mathbf{v}, \boldsymbol{\rho})_{i,j} = \begin{cases} \frac{\rho_{i,j} v_{i,j} - \rho_{i-1,j} v_{i-1,j}}{\rho_{i,j} v_{i,j} + \rho_{i-1,j} v_{i-1,j}}, & \text{if } i > 1 \\ 0, & \text{otherwise} \end{cases} \quad (7)$$

$$S(\mathbf{r})_{ij} = \begin{cases} 0, & \text{if } r_{ij} = 0 \\ 1, & \text{if } |r_{ij}| \geq T \\ 2, & \text{otherwise} \end{cases} \quad (9)$$

$$\mathcal{L}_{\text{boundary}}(\mathbf{v}, \tilde{\mathbf{v}}) = \frac{1}{nm} \sum_{i=1}^n \sum_{j=1}^m W(\mathbf{v})_{ij} G(\mathbf{v}, \tilde{\mathbf{v}})_{ij}$$

$$G(\mathbf{v}, \tilde{\mathbf{v}})_{ij} = |(\nabla_x \mathbf{v})_{ij} - (\nabla_x \tilde{\mathbf{v}})_{ij}| + |(\nabla_z \mathbf{v})_{ij} - (\nabla_z \tilde{\mathbf{v}})_{ij}|$$

Fig. 3. Flowchart of calculating the reflection coefficient tuned factors (a) real velocity map, (b) obtained by (5), (d) obtained by (7), (c) and (e) generated after dilated (b) and (d) according to (6), respectively, (f) Hadamard product of (c) and (e), and (g) obtained by applying (9) on (f).

COMPARISON RESULTS OF THE EVALUATION METRICS ON TEST OpenFWI DATASETS

Dataset	Method	PSNR \uparrow	SSIM \uparrow	UIQ \uparrow	LPIPS ($\times 10^{-3}$) \downarrow	MSE ($\times 10^{-3}$) \downarrow	MAE ($\times 10^{-3}$) \downarrow	BMSE ($\times 10^{-3}$) \downarrow	BMAE ($\times 10^{-3}$) \downarrow
FlatVelA	InversionNet	41.590	0.986	0.852	1.987	0.141	6.527	0.502	9.371
	VelocityGAN	40.951	0.984	0.852	2.769	0.161	6.515	0.408	9.504
	DD-Net70	38.269	0.971	0.854	2.736	0.262	6.954	1.088	13.996
	ABA-FWI	49.105	0.991	0.856	0.310	0.027	2.977	0.083	3.755
FlatFaultA	InversionNet	32.209	0.943	0.836	18.303	0.764	12.160	3.497	29.232
	VelocityGAN	31.258	0.943	0.835	16.985	0.934	12.480	4.418	31.810
	DD-Net70	33.026	0.951	0.842	17.628	0.606	11.566	2.571	26.358
	ABA-FWI	34.977	0.964	0.843	9.887	0.423	8.871	1.923	19.691
CurveVelA	InversionNet	23.280	0.793	0.842	71.505	5.815	37.676	14.915	65.688
	VelocityGAN	23.249	0.802	0.844	66.238	5.825	36.904	15.054	64.518
	DD-Net70	23.519	0.763	0.854	85.501	5.327	41.103	12.273	66.775
	ABA-FWI	24.812	0.850	0.865	32.258	4.073	31.965	10.308	53.147
CurveFaultA	InversionNet	28.335	0.910	0.827	20.201	1.797	16.964	6.933	43.191
	VelocityGAN	26.888	0.859	0.820	25.277	2.430	20.742	8.998	50.574
	DD-Net70	28.086	0.896	0.833	27.089	1.887	19.629	6.442	45.389
	ABA-FWI	29.879	0.911	0.831	15.587	1.297	14.707	4.976	35.452

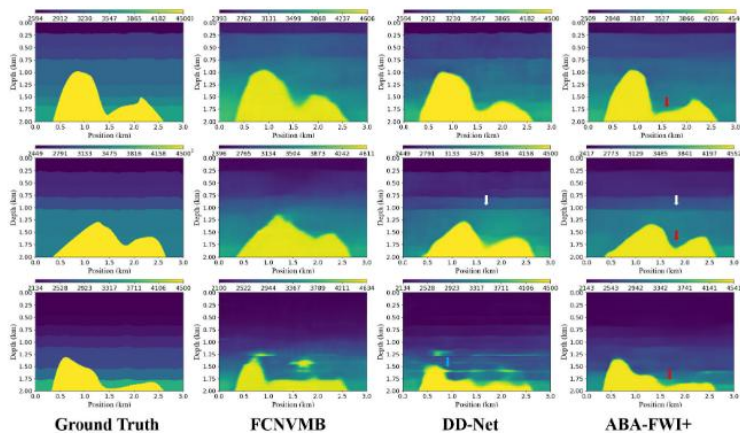


Fig. 8. Inversion results of three methods on three examples from the SEG simulation dataset.

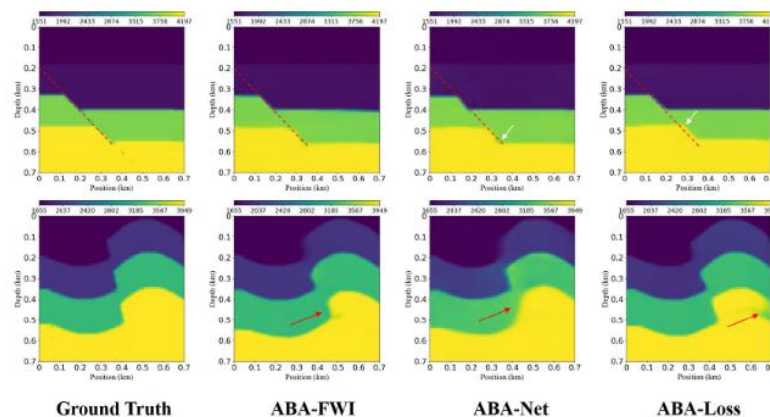


Fig. 11. Comparison of inversion results on whether to use the WTconv layer, SAM, and the RCTB loss. The comparative methods include ABA-Net, ABA-Loss, and ABA-FWI.

Thanks